Electronic Supplementary Material (ESI) for Journal of Materials Chemistry C.

Supplementary Information

Exploiting Supramolecular Assemblies for Filterless Ultra-Narrowband Organic Photodetectors with Inkjet Fabrication Capability

Surendra B. Anantharaman,[*,a,b] *Karen Strassel,*[a,c] *Matthias Diethelm,*[a,b] *Agnes Gubicza,*[d] *Erwin Hack,*[d] *Roland Hany,*[a] *Frank A. Nüesch,*[*,a,b] *and Jakob Heier*[a]

[a] Laboratory for Functional Polymers, Empa, Swiss Federal Laboratories for Materials Science and Technology, Überlandstrasse 129, CH-8600 Dübendorf, Switzerland

[b] Institut des Matériaux, École Polytechnique Fédérale de Lausanne, EPFL Station 12, CH-1015 Lausanne, Switzerland

[c] Institute of Chemical Sciences and Engineering, École Polytechnique Fédérale de Lausanne, EPFL, CH-1015 Lausanne, Switzerland

[d] Transport at Nanoscale Interfaces, Empa, Swiss Federal Laboratories for Materials Science and Technology, Überlandstrasse 129, CH-8600 Dübendorf, Switzerland

Corresponding Authors

* F.A.N (frank.nueesch@empa.ch) or S.B.A (surendrababu87@gmail.com)

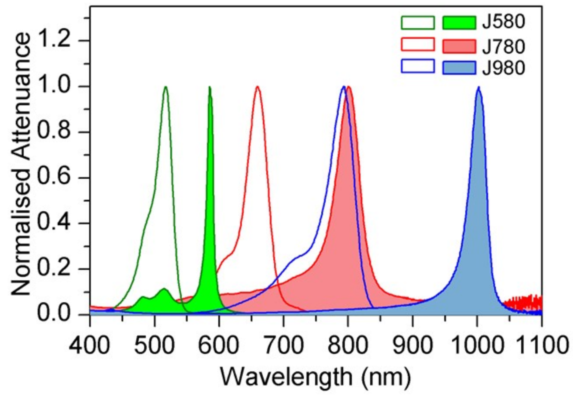

Fig. S1 Normalized monomer (open, in methanol) and J-aggregate (filled) absorption spectra of the three dyes. J-aggregate solutions for **J780** and **J980** were obtained by dispersing the dye in acetate buffer. In the case of **J580**, J-aggregates were obtained by dispersing the dye in water.

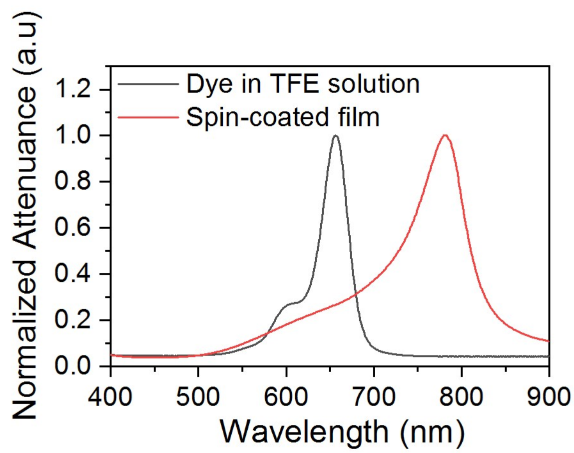

Fig. S2 Attenuance of **J780** dye in TFE solution and in thin film obtained by spin-coating the solution on a glass substrate.

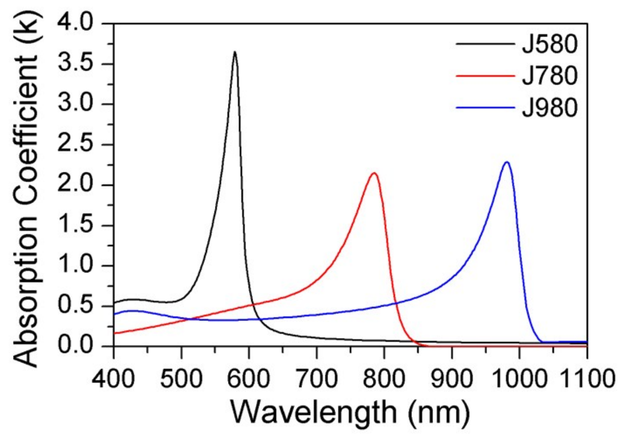

Fig. S3 The extinction coefficients calculated from ellipsometry for J-aggregate thin films spin-coated on TiO_2 coated glass substrates are shown after subtracting the contribution from TiO_2.

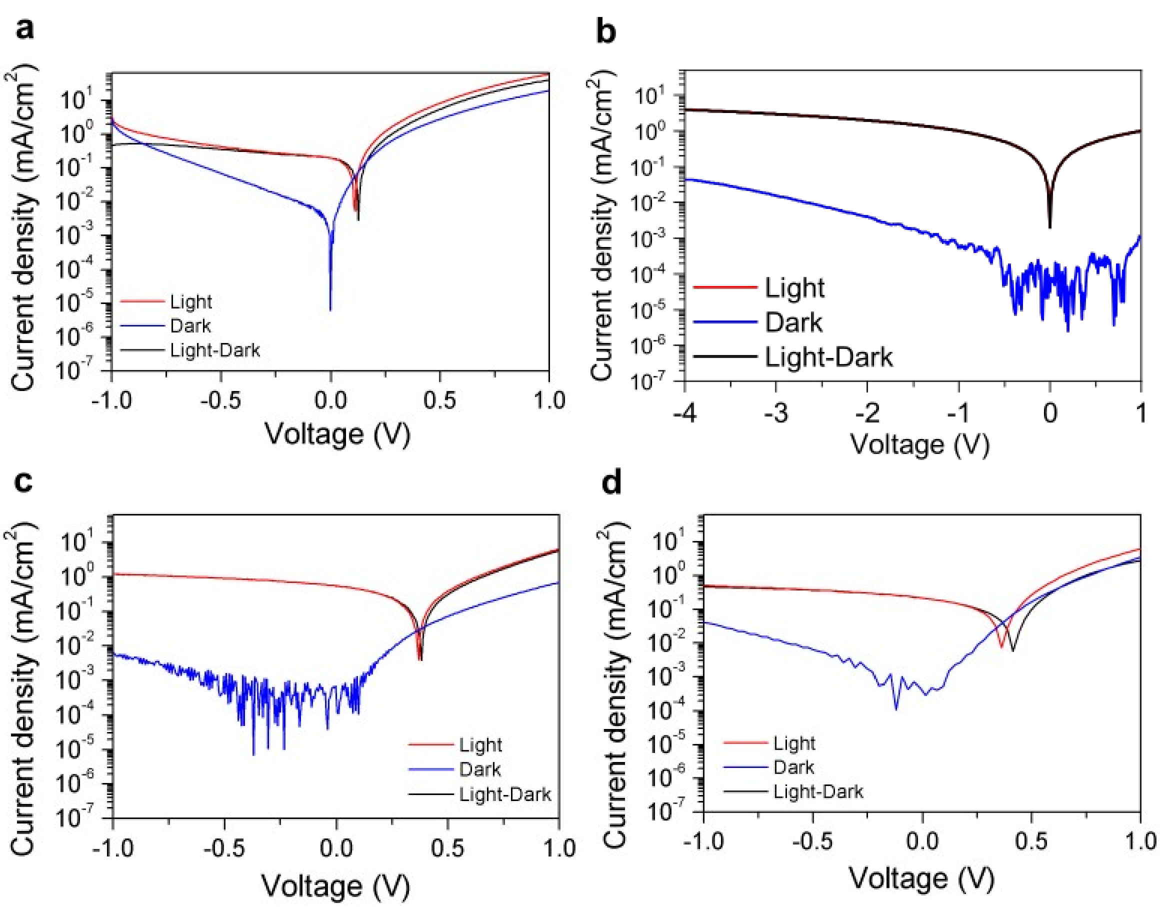

Fig. S4 Log-plots of the current-density – voltage characteristics for the **J580** (a), **J580** with TAPC layer (b), **J780** (c) and **J980** (d) devices measured under simulated solar light (red curves) and in the dark (blue curves). The device structure used is ITO/TiO_2/J-aggregate layer (**J580**, or **J580**+TAPC (50 nm) or **J780** or **J980**)/MoO_3 (10 nm)/Ag (12 nm). For **J580** the direct deposition method was used, while in-situ deposition was used for **J780** and **J980**. The difference between the current-density curves under light and dark, respectively, is indicated as black line.

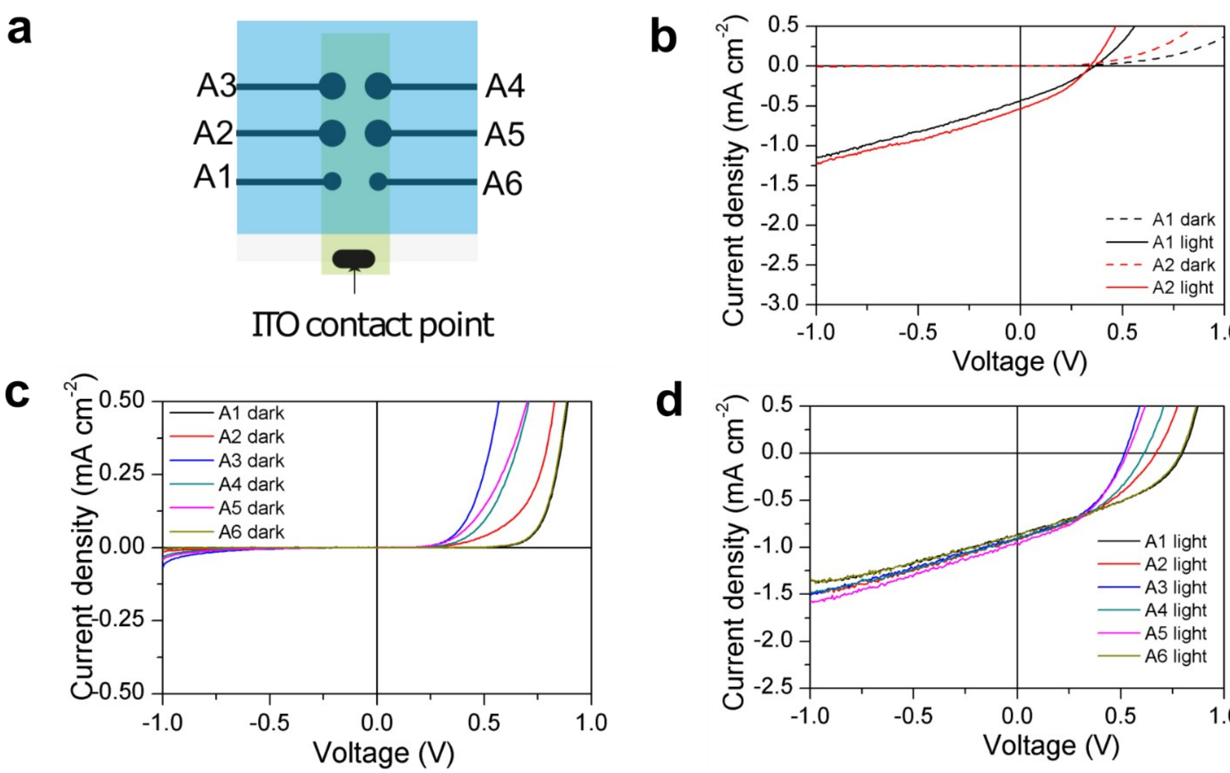

Fig. S5 Schematic of the device (top view) with electrodes (A1 to A6) and ITO contact point (a). Current density-voltage curves for **J780** spin-coated from acetate buffer - direct method (b). In comparison, the J-V curves in the dark (c) and under light (d) are shown for **J780** spin-coated from TFE (in-situ method) for all the six devices.

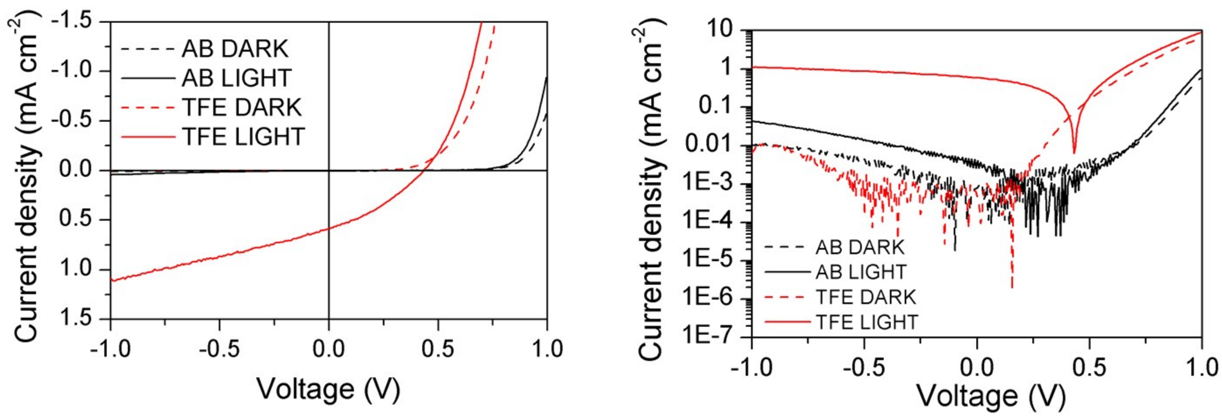

Fig. S6 Comparison of J-V curves for the **J980** devices spin-coated from TFE (in-situ method) and acetate buffer solution (AB, direct method). The best device is reported here for J-aggregate films processed from the acetate buffer solution. The short-circuit current (J_{sc}) showed a 60-fold increase from 0.01 to 0.58 mA cm^{-2} when using the in-situ method. Both the linear scale (left) and logarithmic scale (right) are shown.

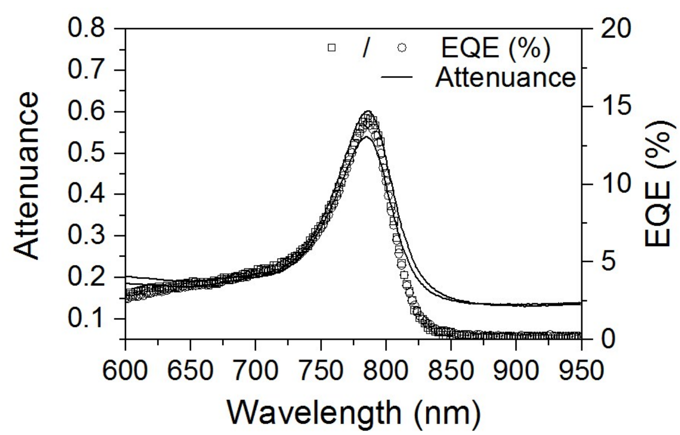

Fig. S7 Attenuance and EQE measured for **J780** devices from two different batches (represented as open square and open circle).

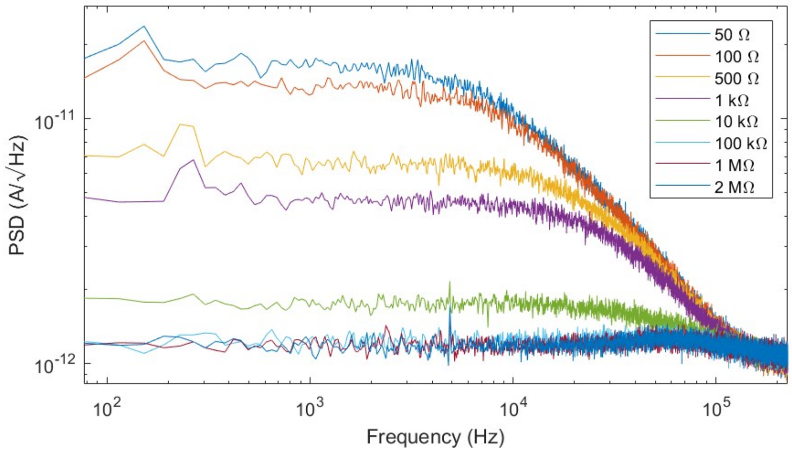

Fig. S8 Noise power spectral density plotted as a function of frequency for standard resistors in the same test fixture.

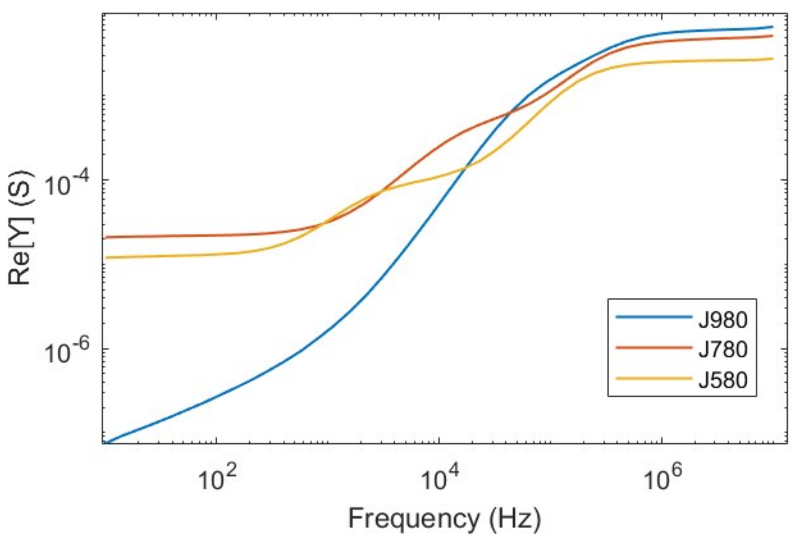

Fig. S9 Real part of the admittance plotted as a function of frequency for **J580**, **J780** and **J980** devices.

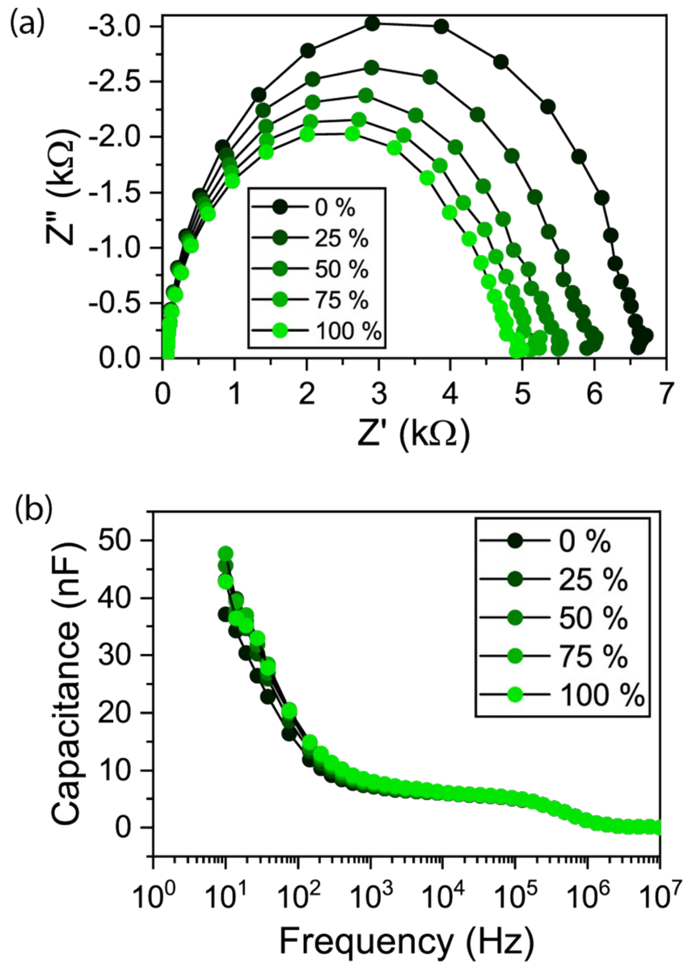

Fig. S10 Impedance (a) and capacitance (b) measured for **J580** devices at 0 V upon illumination with different light intensities.

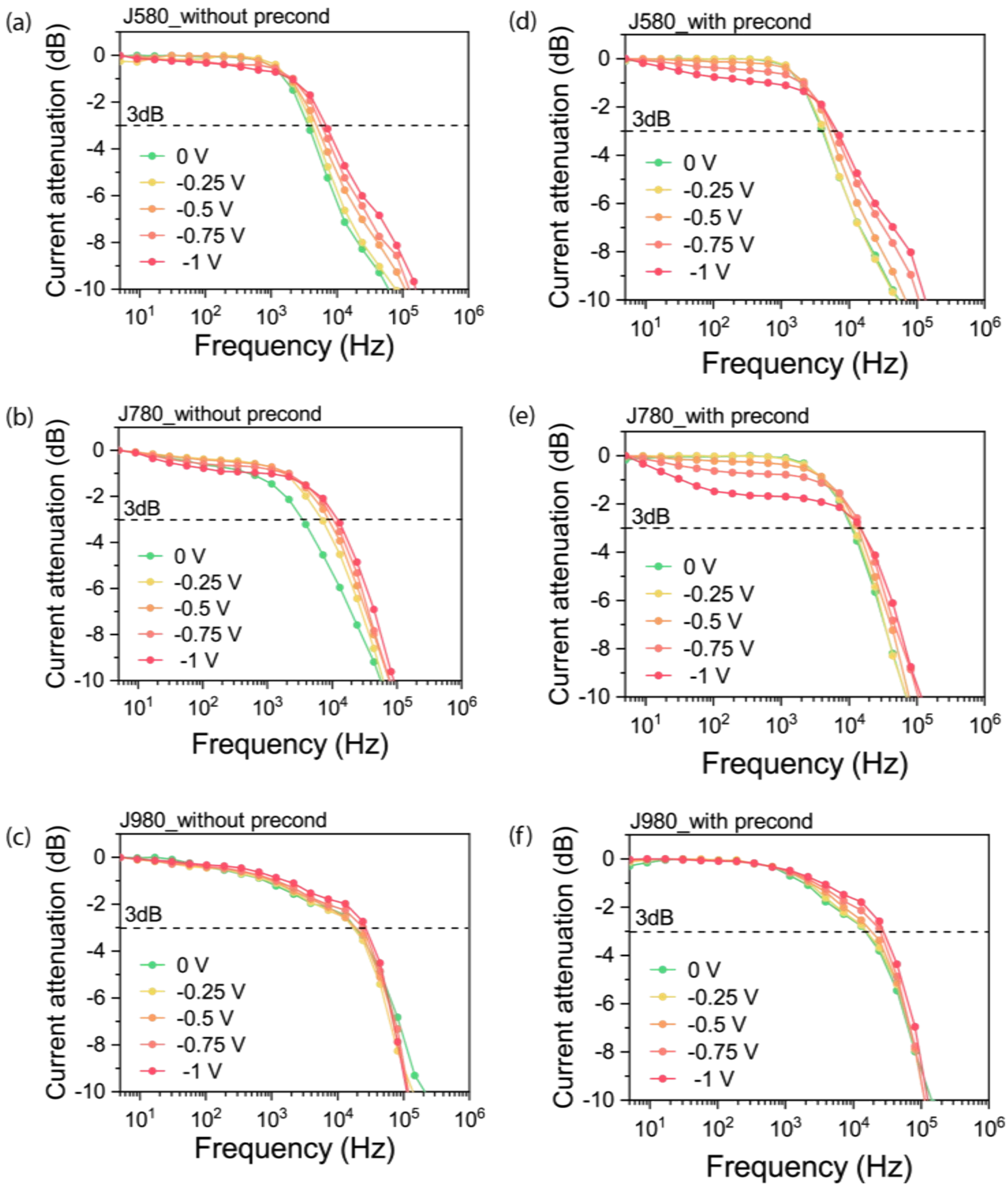

Fig. S11 Frequency response and -3dB values recorded without preconditioning for the **J580** (a), **J780** (b) and **J980** (c) devices and the corresponding values after preconditioning the devices for 120 s at -1 V (d-f).

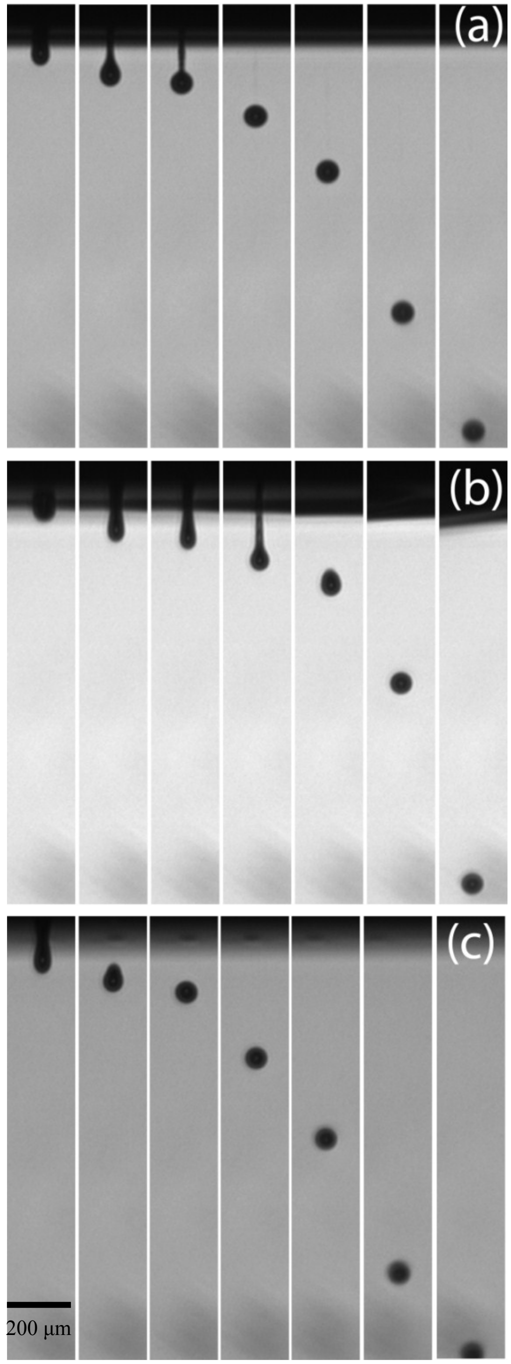

Fig. S12 Stroboscopic images of inkjet drop formation with c-TiO_2 ink (a), m-TiO_2 ink (b) and J-aggregate ink (c) at consecutive intervals (20 μs) after the printing trigger pulse. The elongated tail associated with the ink droplet as observed in (a) and (b) quickly merges with the drop without forming any satellite drops.

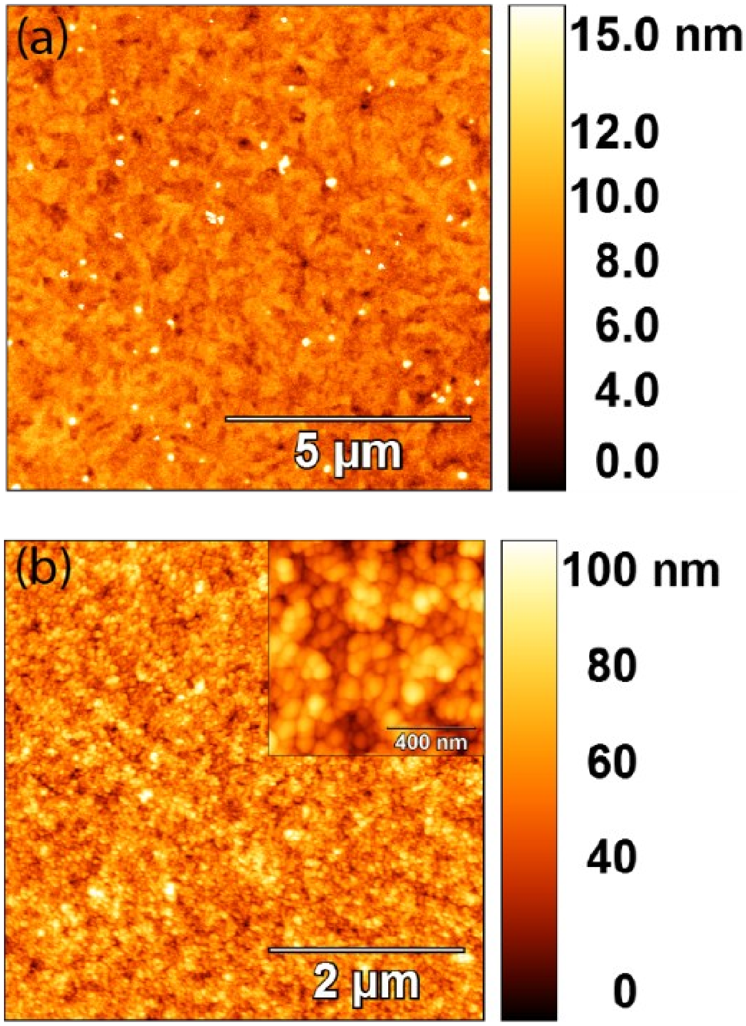

Fig. S13 Topographical images of inkjet printed c-TiO_2 on ITO substrates (a) and m-TiO_2 on c-TiO_2 coated ITO substrates (b).

The relation between thermal noise and resistance

In physical systems in equilibrium, the spectral density fluctuations, for example current noise, and the linear response of the same system to an external perturbation are related. This relation is called fluctuation-dissipation theorem.[1] The thermal motion of charge carriers is a source of random current fluctuations leading to thermal noise. If the noise frequency $\ll \frac{k_B T}{h}$, one can derive the relation between the current noise spectral density $S_I(f)$ and the complex impedance $Z(f)$:

$$S_I(f) = 4k_B T Re(\frac{1}{Z(f)}) \qquad (1)$$

Here k_B is the Boltzmann-constant, T is the temperature, and $Re(Z(f))$ is the real part of the impedance, i.e the resistance. If the resistance is frequency-independent, which is usually the case for conventional resistors, equation (1) simplifies to the well-known expression of

$$S_I(f) = \frac{4k_B T}{R} \qquad (2)$$

describing a frequency-independent, flat white noise. However, in our case $Z(f)$ heavily varies with frequency, hence according to equation (1), the frequency-dependence of the impedance is also reflected in the current noise spectrum.

Reference

1. S. Kogan, *Electronic noise and fluctuations in solids*, Cambridge University Press, 1996.